Available online at www.sciencedirect.com

ScienceDirect

Procedia Engineering 161 (2016) 990 – 1000

Procedia Engineering

www.elsevier.com/locate/procedia

World Multidisciplinary Civil Engineering-Architecture-Urban Planning Symposium 2016, WMCAUS 2016

Numerical Investigation of Structural Behaviour of Timber-Glass Composite Beams

Marcin Kozłowski[a,b,*], Marta Kadela[c], Jacek Hulimka[a]

[a] *Silesian University of Technology, Department of Structural Engineering, ul. Akademicka 5, 44 -100 Gliwice, Poland*
[b] *Eckersley O'Callaghan Ltd, 9th Floor, 236 Gray's Inn Road, London WC1X 8HB, UK*
[c] *Building Research Institute - Silesian Branch, al. Korfantego 191, 40-153 Katowice, Poland*

Abstract

The current trends in modern architecture are focused on minimising the boundaries between the external environment and interior of the building. This requires a continuous increase of the amount of translucent surfaces allowing natural sunlight to enter the building, not only in facades but also through interior structural elements. The research project on timber-glass composite beams is based on an assumption that timber and glass work together to carry external loads. Glass no longer acts as a filling, as in traditional solutions, but actively participates in load transfer. The paper presents result of numerical study on modelling of brittle failure (cracking) of glass. The influence of element geometry, element size and value of fracture energy on the structural performance were analysed. From these studies the optimum model parameters were chosen for final models of timber-glass composite beams. Subsequently, the models were validated by comparing their results with experimental studies.

Peer-review under responsibility of the organizing committee of WMCAUS 2016

Keywords: timber-glass composite; beams; brittle materials, brittle failure;

1. Introduction and previous work

Timber and glass have been widely used in many architectural applications. Solutions such as glass panes bonded to timber frames have been known for many years. However, the traditional solutions assume that glass only fills the frame and its main role is to transfer wind load to the structural frame. In practice glass with its high strength and

* Corresponding author. Tel.: +48-32-237-22-88; fax: +48-32-237-22-88.
E-mail address: marcin.kozlowski@polsl.pl

Peer-review under responsibility of the organizing committee of WMCAUS 2016
doi:10.1016/j.proeng.2016.08.838

stiffness may highly contribute to the system. The research project, presented in the paper, is based on a different assumption - namely, that timber and glass work together to carry external loads. It combines high stiffness of glass and ductile nature of timber. Furthermore, the idea focuses on the possibility to overcome the drawbacks inherent in glass – its brittle behavior at failure and relatively low tensile strength. This idea opens up new perspectives for architects – timber framing can be thinner, making facades lighter and more impressive, see Fig. 1.

Fig. 1 Timber-glass composite beams as structural members of roof structure and conservatory (architectural visualizations).

The current knowledge about synergetic features of timber-glass composites relates to a few previously conducted research projects within last fifteen years. Early examples of timber-glass composites were presented in the mid and late 1990s and early 2000s [1-3]. More detailed research was made by several researchers [4-17]. The concept developed by Kreher was applied in the roof structure of the Palafitte Hotel in Monruz (Switzerland), [6]. Numerical simulation of glass beams, in particular glass fracture, has been investigated before. The first approaches of these investigations used plane-stress methods that required implementation of computational code [18-21]. Results of more advanced models using ABAQUS platform and *brittle cracking* material model (also applied in the research presented in the paper) were presented in [22-24]. The paper presents numerical research on timber-glass composite beams with focus on the modelling of brittle failure of glass. The influence of element geometry, element size and fracture energy of glass on results were investigated. Finally, models with optimum parameters were validated by using experimental data.

2. Numerical model

2.1. Geometry

Fig. 1a presents the cross-section of the analyzed beam. The beam was 300 mm high and 1800 mm long. The glass web measured 8×200 mm and the timber flanges measured 45×75 mm in cross section. Groove measuring 13×30 mm allowed for 2.5 mm bond on both sides of the glass web. Fig. 2b-c show that only a quarter beam was taken into account with appropriate boundary conditions simulating a four-point bending test, due to the symmetries of the beam, Load introduction points and supports were modelled using 50 mm long rigid surfaces that ensured distribution of forces to larger number of elements.

All components were modelled using 3D solid elements. For the flanges and bond connections 8-node linear brick elements (C3DR8) with reduced integration and large strain formulation were used. For the web, two types of elements were used: 8-node linear brick elements (C3DR8) with reduced integration and large-strain formulation and 6-node linear triangular prism elements (C3D6). In all models, 5 mm and 2 mm element size was applied for the flanges and adhesive connection, respectively. All calculations were run in displacement control including non-linear effects of large deformations. The displacement was increased linearly using a smooth amplitude function.

2.2. Materials

Mechanical properties of materials used in the study are presented in Table 1.

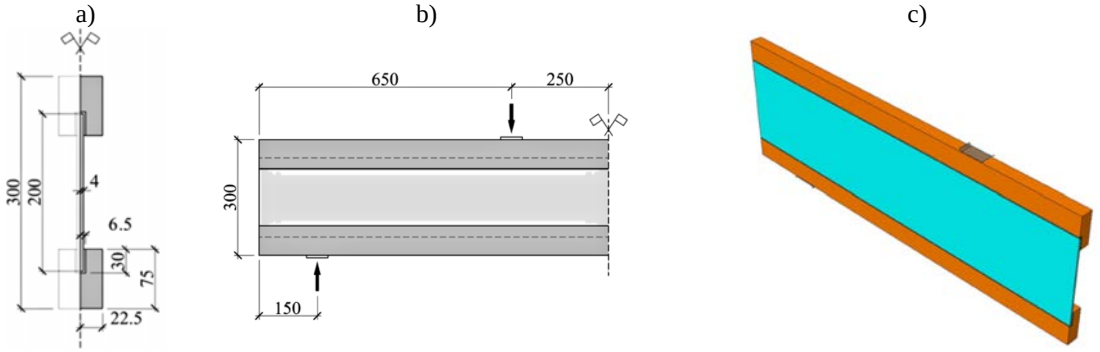

Fig. 2 Model of timber-glass composite beam: (a) cross-section, (b) loading introduction points and boundary conditions, (c) 3D model.

Glass was modelled with isotropic and linear elastic material properties. The values of modulus of elasticity E and maximal tensile stress ft were determined based on experimental results [17]. The value of Poisson's ratio ν was taken from the literature [25]. To model brittle failure of glass, a smeared crack model along with *brittle cracking* and *brittle failure* damage evolution sub-options were used [29]. In this approach, a crack initiation is governed by the maximal tensile stress f_t and crack propagation is based on the fracture energy of glass G_f. The value of G_f was preliminary set equal to 3.0 J/m^2 after [27]. Based on f_t and G_f a crack normal displacement δ_u was calculated according to the formula $\delta_u = 2 \times (G_f / f_t)$. Post-cracking behaviour (decrease of shear modulus with crack opening) was modelled using the shear retention model. The values of $\varepsilon_{crack,max}$ were calculated taking into account the size of finite elements. In the analyses it was assumed after [26] $\varepsilon_{crack,max} = 2 \times \varepsilon_{crack(u)}$.

Timber was modelled with orthotropic, linear elastic material properties. The values of modulus of elasticity E_1 (modulus of elasticity along the fibers) was determined experimentally [17] while remaining parameters were calculated proportionally based on literature.

Adhesives were modelled with isotropic, linear elastic material properties. Mechanical properties of adhesives used in the research were investigated in [17].

Table 1 Mechanical properties of materials

Material	Modulus of elasticity [MPa]			Poisson's ratio [-]			f_t [MPa]	G_f [J/m^2]
Glass	E = 70 000			ν = 0.23			45.0	3.0
Timber	E_1 = 10540	E_2 = 750	E_3 = 750	ν_1 = 0.44	ν_2 = 0.40	ν_3 = 0.52	-	-
Acrylate adhesive	E = 78			ν = 0.46			-	-
Silicone adhesive	E = 3			ν = 0.46			-	-

2.3. Methods

All numerical simulations were performed using the finite element software ABAQUS and Explicit solver [29]. To find the optimum model parameters some factors were varied to investigate their effect on the numerical results. The simulations were performed according to the beam model bonded with acrylate adhesive with groove dimensions of 13×30 mm due to the computational cost of analysis. Variations of model parameters are presented in Table 2.

Firstly, the geometry of the finite elements was varied. Since the smeared model is susceptible to elements shape, the geometry of the elements was varied between rectangular and prism with triangular base elements, see Fig. 3. Secondly, the size of rectangular and prism elements were altered among 8, 4 and 2 mm, see Fig. 3. The value of 8 mm corresponds to the thickness of glass used in the experimental research to validate numerical models. Finally,

the fracture energy of glass varied between 3.0 and 8.0. J/m^2, these values were reported in [27] and [28], respectively. To check sensitivity of results, an intermediate value of 5.5 J/m^2 was considered.

Table 2 Overviefw of parameters of numerical models

Variation	Model	Element geometry	Element size [mm]	Fracture energy G_f [J/m^2]
Element type and element size	P-01	rectangular	8.0	3.0
	P-02		4.0	
	P-03		2.0	
	P-04	prism	8.0	
	P-05		4.0	
	P-06		2.0	
Fracture energy of glass	P-07		4.0	5.5
	P-08		4.0	8.0

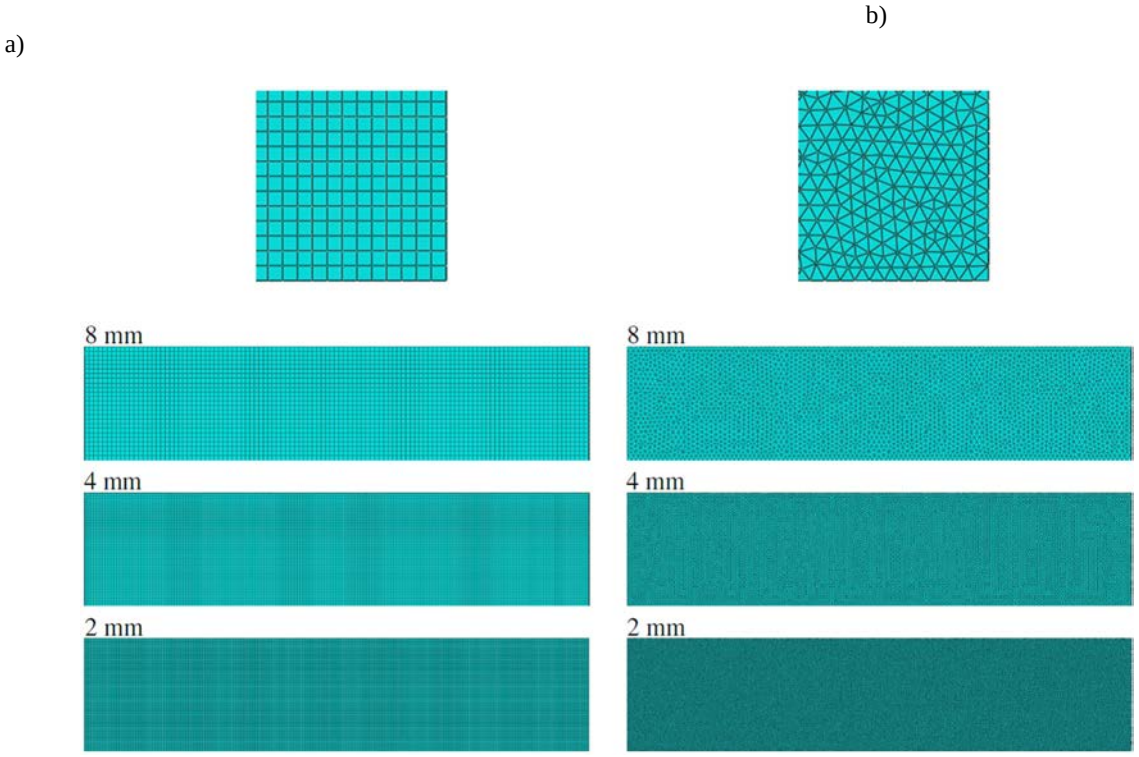

Fig. 3 Element sizes used in parametric studies: (a) rectangular elements, (b) prism elements.

3. Results and discussion

To ensure the quasi-static response of the numerical models the ratio of kinetic energy to the internal strain energy must be kept at <5% during entire analysis [30]. Before any numerical results were accepted, the ratio was evaluated so that it showed <5%.

ABAQUS/Explicit solver is a dynamic analysis solver and dynamic effects such as oscillation cannot be avoided. Thus, the results obtained from numerical analysis were smoothed using a smoothing function available in ABAQUS to eliminate the oscillation effect.

3.1. Variation of element geometry and element size

Regarding the variation of element geometry and element size, models P-02÷06 were investigated and compared to the reference model P-01. In terms of the load-displacement curves, the results present small differences, see Fig. 4. For all models in the first stage the relationship between the load and vertical mid-span displacement is almost perfectly linear until initial cracking. This is followed by a sudden drop of bending stiffness and an increase of vertical displacement. Initial cracking of glass web, for all models, occurs at the same load of approximately 29 kN and displacement of 1.8 mm. Subsequently, the existing crack propagates and at the load of approximately 65 kN the next crack is formed. The ultimate failure of all models occurs at the load of 120-142 kN and displacement of 16-20 mm.

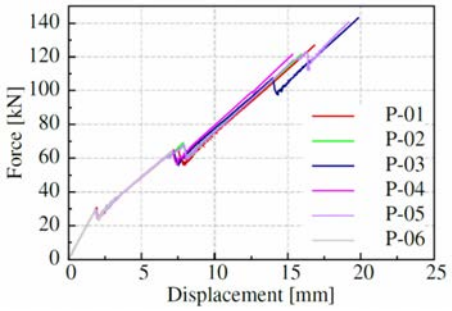

Fig. 4 Load-displacement plots for numerical models P-01÷06.

Despite close results regarding load-displacement curves, mesh refinement does significantly alter the cracking pattern. Fig. 5÷Fig. 7 show cracking pattern for numerical models P-01÷06 with variable geometry and size of finite elements. Two element types (brick and prism element) and three element sizes (8, 4 and 2 mm) were considered. Models with a coarse mesh (8 mm) show a relatively limited number of cracks when compared to the models with finer mesh (4 and 2 mm). It can be explained that the higher number of elements; the more cracking originates in the model. In terms of the element type, models with brick elements show a relatively limited number of cracks, while models with prism elements demonstrate more extensive cracking. Moreover, the models with prism elements show presence of diagonal cracks. The model P-06 with 2 mm prism elements displays the fracture pattern of the glass web similar to the beam investigated experimentally [11,17].

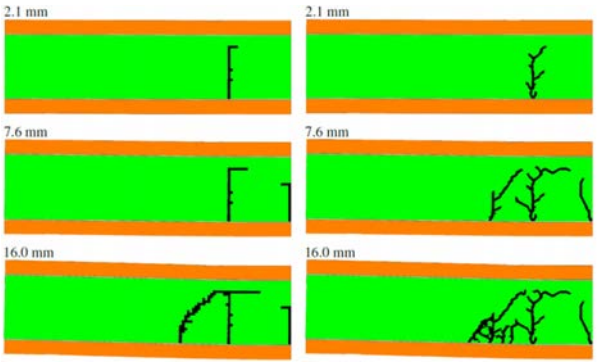

Fig. 5 Crack pattern for numerical models P-01 and P-04 at different displacement.

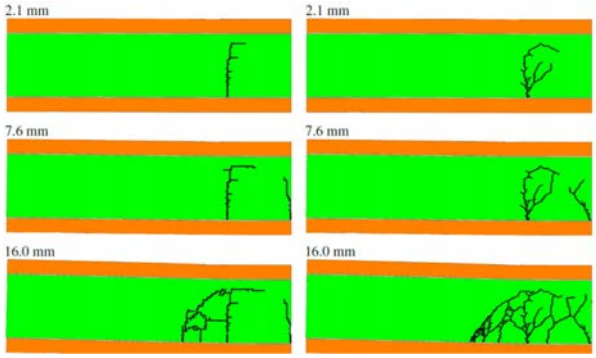

Fig. 6 Crack pattern for numerical models P-02 and P-05 at different displacement.

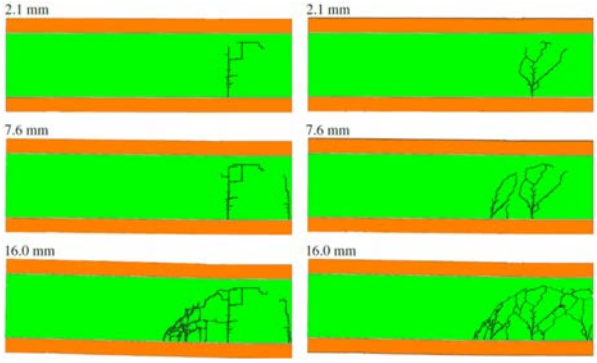

Fig. 7 Crack pattern for numerical models P-03 and P-06 at different displacement.

3.2. Variation of fracture energy

A comparison obtained from models P-05, P-07 and P-08 is presented in Fig. 8 and Fig. 9. Variation of the value of the fracture energy of glass does not alter numerical results and, no significant effects were found in the global resistance and structural performance. However, major discrepancies were found in cracking pattern. Regarding load-displacement behavior the results of these models are similar until second crack in glass occurs, see Fig. 8. From this point the models present small differences in the occurrence of subsequent cracks. However, the global performance is similar and ultimate failure occurs at the same displacement. In terms of cracking patterns, the increase of fracture energy, in general, results in a decrease of number of cracks in glass, see Fig. 9. The cracking model P-05 shows the fracture pattern of the glass web similar to the beam investigated experimentally [11,17].

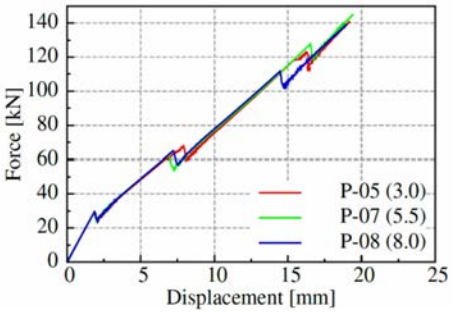

Fig. 8 Load-displacement plots for numerical models P-05, P-07 and P-06.

From the parametric analyses it is concluded that variation of model parameters assumed does not alter significantly the results. In terms of load-displacement plots, the results of type and size of elements present minor differences regarding the load and displacement at ultimate failure. In terms of cracking pattern models with larger number of elements (fine mesh with prism elements) results in larger number of cracks which correspond to the results observed in experimental investigations [17]. Similar to the effect of type and size of elements, the variation of fracture energy does not change the load-displacement plots. However, the increase of fracture energy results in decrease of number of cracks.

Based on the findings from parametric studies the final models were built. Taking into account the load-displacement curves, crack patter and computational cost the optimum model parameters were: prismatic element type, element size 4 mm and fracture energy of glass 3.0 J/m^2. Final models are indicated as F-SSB-01÷02 and F-SSB-03÷04 and bonded with acrylate and silicone adhesive, respectively. Different models with varying width of the grooves correspond to the specimens investigated experimentally.

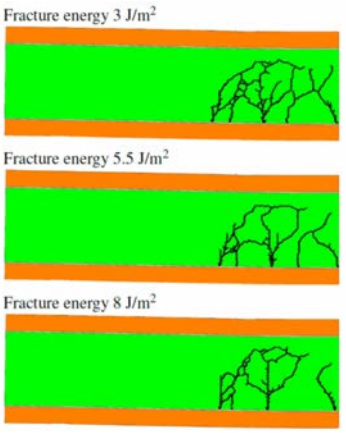

Fig. 9 Crack pattern for numerical models P-05, P-07 and P-08 with varying value of fracture energy of glass at displacement of 12.4 mm.

3.3. Validation with experimental results

This section presents a comparison of the numerical predictions and test results of timber-glass composite beams bonded with acrylate and silicone adhesives. The specimens are indicated as BA1÷3 and BS1÷2, respectively.

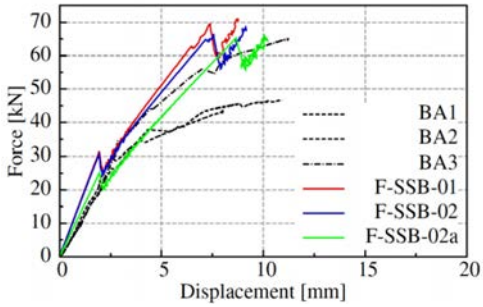

Fig. 10 Load-displacement plots obtained from experimental and numerical analyses of timber-glass beams bonded with acrylate adhesive.

Fig. 10 and Table 3 present the results of numerical investigations compared to the experimental testing of beams bonded with acrylate adhesive. The numerical results are in fairly good agreement with the experimental results. Despite different geometry of the groove, no difference in the initial stiffness and load at first glass cracking between models F-SSB-01 and F-SSB-02 can be observed. The curves start diverging from the load of approximately 60 kN, when shear cracks form. At this stage, due to the large strain in the adhesive different behaviour is observed. The stiffness of the bond line connection is caused due to the wider groove and larger volume of adhesive which allows for greater deformations in model F-SSB-02 as compared to model F-SSB-01.

Table 3 Experimental and numerical results of timber-glass beams bonded with acrylate adhesive (F_{crack} corresponds to the level of load at first cracking).

Model	Experimental		Numerical	
	F_{crack} [kN]	EI_{exp} [MNm^2]	F_{crack} [kN]	EI_{num} [MNm^2]
F-SBB-01	27.9	0.658	31.4 (+12.5%)	0.966 (+46.8%)
F-SBB-02	26.4	0.632	30.6 (+15.8%)	0.941 (+48.9%)
F-SBB-02a	26.4	0.632	25.3 (-4.3%)	0.779 (+23.3%)

For both models (F-SSB-01 and F-SSB-02) the initial stiffness obtained from the numerical analyses overestimate the results from experiments, see Table 3. This can be explained by the fact that the actual stiffness of the acrylate adhesive is lower than the one obtained from the testing of the adhesive in tension [17], even for the lowest load rate. For numerical models F-SSB-01 and F-SSB-02, the load at first cracking in glass and initial stiffness are approximately 14 % and 48 % higher, respectively, as compared to the experiments. Therefore, additional model F-SB-02a with reduced modulus elasticity of acrylate adhesive was computed and the corresponding initial bending stiffness was evaluated. The reduced value of the modulus of elasticity (E=17 MPa) corresponds to the results of relaxation tests on acrylate adhesive [17]. The results of the model F-SSB-02a are in much better agreement (regarding the initial bending stiffness and the load at first cracking) with the experimental results. In this case, when compared to experimental results, the load which causes first cracking in glass is approximately 4% lower and the initial bending stiffness is 23% higher. The numerical models simulate correctly the ultimate failure of the beams. During the testing it was observed that the final failure was caused by the failure of the flange working in tension. Thus the numerical calculations were stopped at the stage when tensile stress in the timber flanges exceeds the ultimate tensile stress obtained from experimental investigation on timber specimens in four-point bending [17]. In terms of crack pattern, numerical models were simulated accurately with the tested beams [18]. No differences regarding crack patterns between models F-SSB-01, F-SSB-02 and F-SSB-02a were observed.

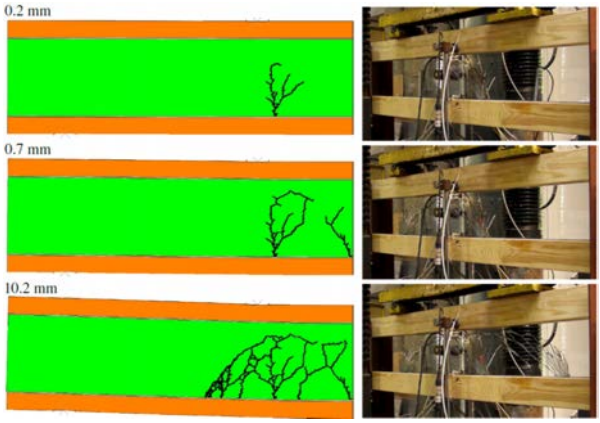

Fig. 11 Cracking pattern at different displacement obtained from numerical analysis and observed during experiments for beam bonded with acrylate adhesive.

Fig. 12 and Table 4 present the results of numerical investigations and experimental testing of timber-glass composite beams with silicone adhesive. From Fig. 12 it can be seen that the numerical results are in very good agreement with the experimental results. Despite different geometry of the groove, no difference in the initial stiffness and load at glass cracking between models F-SSB-03 and F-SSB-04 can be observed. The curves start diverging from the point when first crack occurs. At this stage due to large strain in the adhesive different behaviour is observed. The stiffness of the bond line connection, due to wider groove, allows for greater deformations in model F-SSB-04 as compared to model F-SSB-03. In terms of the load at first cracking in glass, the numerical models underestimate the experiments by approximately 10%, see Table 4. However, regarding the initial stiffness, the numerical models overestimate the results from the experiments by approximately 7%. The numerical models simulate correctly with the ultimate failure of the beams. During testing it was observed that the final failure was caused by the failure of the flange working in tension. Thus the numerical calculations were stopped at the stage when the tensile stress in the timber flanges exceeds the ultimate tensile stress obtained from experimental investigation on timber specimens in four-point bending [17].

In terms of cracking pattern, the numerical models are in good agreement with the experimental results. From both methods, only one crack located in the center of the specimen was observed, see Fig. 13.

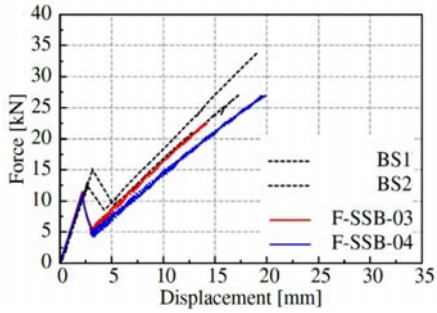

Fig. 12 Load-displacement plots obtained from experimental and numerical analyses of timber-glass beams bonded with acrylate adhesive.

Table 4 Experimental and numerical results of timber-glass beams bonded with silicone adhesive (F_{crack} corresponds to the level of load at first cracking).

Model	Experimental		Numerical	
	F_{crack} (*kN*)	EI (*MNm2*)	F_{crack} (*kN*)	EI (*MNm2*)
F-SBB-03	12.7	0.292	11.5 (-9.5%)	0.315 (+7.9%)

F-SBB-04	12.6	0.289	11.1 (-11.9%)	0.307 (+6.2%)

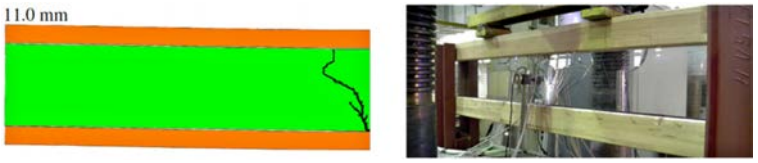

Fig. 13 Cracking pattern at different displacement obtained from numerical analysis and observed during experiments for beam bonded with silicone adhesive.

4. Conclusions

In this paper the results of numerical modelling of the structural response of timber-glass composite beams were presented. Firstly, parametric studies were performed to find the optimum model parameters for final models. Subsequently, the models were validated with experimental results.

From the parametric investigations it is concluded that Explicit solver and Brittle cracking feature, available in ABAQUS software, offer a suitable technique for simulating the cracking of glass. Regarding the effect of the element geometry and element size on the numerical results, it is concluded that the parameters do not affect the response of the model in terms of load-displacement plots. The same observation was made for models with varying fracture energy of glass. However, mesh refinement does significantly alter the cracking pattern. The models with larger number of elements result in a larger number of cracks. In terms of the element type, models with rectangular brick elements show a relatively limited number of orthogonal cracks while models with prism shape elements demonstrate more extensive cracking and diagonal cracks. It was also observed that the increase of fracture energy results in decrease number of cracks. Considering calculation time, load-displacement plots and cracking pattern 4 mm prism elements with the value of fracture energy of 3.0 J/m^2 are the optimum combination of parameters.

The results of final models correspond to the results of the experimental campaign. In terms of number of cracks and cracking pattern in the glass web, the numerical simulations are in very good unison with the experiments. However, in the case of the beams bonded with acrylate adhesive, which shows visco-elastic behaviour, additional test must be carried out to obtain real characteristics of the material.

References

[1] W. Stiell, J. Schmid, K. Lieb, H. Krause, F. Stengel, Geklebte Glaselemente in Holz-tragwerken. Abschlußbericht. Institut für Fenstertechnik, Rosenheim, 1996.
[2] J. Schmidt et al., Einsatz von geklebten Glaselementen bei Holztragwerken - ein Beitrag zur Innovation in der Holz-bauarchitektur (Objektversuche). Institut für Fenstertechnik, Rosenheim, 1998.
[3] J. Natterer et al., New joining techniques for modern architecture, in: Rosenheimer Fenstertage, 2002.
[4] J. Hamm, Tragverhalten von Holz und Holzwerkstoffen im statischen Verbund mit Glas, PhD thesis, École Polytechnique Fédérale de Lausanne, 1999.
[5] J. Hamm, Development of Timber-Glass Prefabricated Structural Elements, in: Innovative Wooden Structures and Bridges IABSE, Conference Report 85, Lahti, 2001, pp. 41-46.
[6] K. Kreher, K., Tragverhalten und Bemessung von Holz-Glas-Verbundträgern unter Berücksichtigung der Eigenspannungen im Glas, PhD thesis, École Polytechnique Fédérale de Lausanne, Lausanne, 2004. (in German)
[7] K. Kreher, K., Load Introduction with Timber Timber as Reinforcement for Glued Composites (Shear-Walls, I-Beams). Structural Safety and Calculation-Model, in: 9th World Conference on Timber Engineering, Conference Proceedings, Portland, 2006.
[8] P. Cruz, J. Pequeno, Timber-Glass Composite Beams: Mechanical Behaviour & Architectural Solutions, in: Challenging Glass Conference 1, Conference Proceedings, Delft University of Technology, Delft, 2008.
[9] L. Blyberg, E. Serrano, Timber/Glass Adhesively Bonded I-beams, in: Glass Performance Days, Conference Proceedings, Tampere, 2011.
[10] M. Kozłowski, Hybrid glass beams. Review of research projects and applications, in: ACEE Journal 5(03) (2012).
[11] M. Kozłowski, J. Hulimka, Load-bearing capacity of hybrid timber-glass beams, in: ACEE Journal 7 (02) (2014).
[12] L. Blyberg, M. Lang, K. Lundstedt, M. Schander, E. Serrano, M. Silfverhielm, C. Stalhandske, Glass, timber and adhesive joints - innovative load bearing building components, in: Constr. Build. Mater. 55 (2014) 470–478.
[13] M. Premrov, M. Zlatinek, A. Strukelj, Experimental analysis of load-bearing timber-glass I-beam, in: Constr. Unique Build. Struct. 4 (19), (2014) 11-20.

[14] M. Dorn M, M. Kozłowski, E. Serrano, Development of large-scale load-bearing timber-glass structural elements, in: World Conference on Timber Engineering, Conference Proceedings, Quebec City, 2014.
[15] M. Kozłowski, E. Serrano, B. Enquist, Experimental investigation on timber- glass composite I-beams, in: Challenging Glass 4 and COST Action TU 0905 Final Conference, Conference Proceedings, Lausanne, 2014.
[16] M. Dorn, M. Kozłowski, E. Serrano, Design approaches for timber-glass beams, in: Engineered transparency, International Conference at Glasstec, Conference Proceedings, Düsseldorf, 2014.
[17] M. Kozłowski, Experimental and numerical analysis of hybrid timber-glass beams, PhD thesis, Silesian University of Technology, Gliwice, 2014.
[18] J.H. Nielsen, J.F. Olesen, Mechanically Reinforced Glass Beams, In: Recent Developments in Structural Engineering, Mechanics and Computation, Conference Proceedings, Cape Town, 2007, pp. 655–657.
[19] A.B. Olgaard, J.H. Nielsen, J.F Olesen, Design of Mechanically Reinforced Glass Beams - Modelling and Experiments, in: Structural Engineering International 19 (2) (2009) 130–136.
[20] C. Louter, A. Van de Graaf, J. Rots, Modeling the Structural Response of Reinforced Glass Beams using an SLA Scheme, in: Challenging Glass 2, Conference on Architectural and Structural Applications of Glass, Conference Proceedings, 2010.
[21] J.R. Correia, L. Valarinho, F.A. Branco, Ductility and post-cracking strength of glass beams strengthened with GFRP pultruded composites, in: Composite Structures 93 (9) (2011) 2299–2309.
[22] C. Bedon, C. Louter, Parametric 2D numerical investigations of the structural response of SG-laminated reinforced glass beams, in: Challenging Glass 4 & COST Action TU0905 Final Conference, Conference Proceedings, 2014.
[23] C. Bedon, P.C. Louter, Exploratory numerical analysis of SG-laminated reinforced glass beam experiments, Eng. Struct. 75 (2014) 457-468.
[24] K. Martens, R. Caspeele, J. Belis, Numerical investigation of two-sided reinforced laminated glass beams in statically indeterminate systems, Glass Structures & Engineering (2016) 1-15.
[25] EN 572-2:2012 Basic soda lime silicate glass products - Part 2: Float glass.
[26] I.V. Ivanov, T. Sadowski, Efficient finite element models of laminated glass structures subjected to low-velocity impact, in: Challenging Glass 4, Conference Proceedings, 2014, pp. 499–506.
[27] M. Haldimann, A. Luible, M. Overend, Structural Use of Glass, IABSE, 2008.
[28] F. Bernard, B. Krour, B. Fahsi, Analysis of the debonding risks and the failure of laminated glass thanks to a coupled analytical-numerical investigation, in: COST Action TU0905 Mid-term Conference on Structural Glass, Conference Proceedings, 2013, pp. 391–403.
[29] D. Hibbit, B. Karlsson, P. Sorensen, ABAQUS/Standard User's Manual Ver. 6.10, Pawtucket, Rhode Island, 2004.
[30] W.J. Chung, J.W. Cho, T. Belytschko, On the dynamic effects of explicit FEM in sheet metal forming analysis, in: Engineering Computations 15 (6) (1998), pp. 750–776.